

Single Control Surface UAV Report

AEM 4331/4333: Senior Design/Build

Advisors: Professor Peter Seiler and Raghu Venkataraman

Team Lead: Aaron Krause

Team Members:

Ryan Condrón

Emery Day

Derek Dessens

Parks Wagner



From left to right: Derek Dessens, Emery Day, Parks Wagner, Ryan Condrón, and Aaron Krause

Contents

1	Introduction	1
2	Design and Analysis	1
2.1	Requirements	1
2.2	Conceptual Design of Aircraft	2
2.3	Performance Analysis	12
2.4	Control Surface Sizing and Placement	12
3	Build	14
3.1	Build Readiness Review	14
3.2	Component Selection and Sizing	14
3.3	Build Details	17
3.4	Final Weight and Moment of Inertial Swings	23
4	Flight	26
4.1	Flight Readiness Review	26
4.2	Pre Flight Checklist (Before Departure)	27
4.3	Pre Flight Checklist (On Site)	29
4.4	Flight Tests	31

1 Introduction

Failure of a control surface is one of the fastest ways for a UAV to experience catastrophic loss of control. To have a UAV capable of continuing controlled flight after control surface failure would allow a higher standard of reliability and go a long way towards bringing UAVs into the U.S. Airspace

The goal of this project was to design and build a piloted UAV that was able to land safely after the in-flight failure at trim of one of the two control surfaces. The UAV should maximize nominal flight performance while retaining the ability to remain controllable in flight with a failed control surface.

2 Design and Analysis

2.1 Requirements

Requirements were initially set on the assumption that the UAV would operate by taking video over farmland and attempted to mirror specifications of UAVs that currently fulfilled that role.

Altitude	200 ft
Cruise Velocity	40 mph
Descent Rate	Safe Landing
Endurance	20 mins
Payload	2 lbs
Span	6 ft
Turn Radius	440 ft

Table 1: Table of design requirements

Altitude was based on an estimation of what a high resolution camera would be able to take and still see details. Cruise velocity was based off an operating Reynolds number of 450,000 which would allow the airfoil to operate as desired. Descent rate was left unspecified with the condition of safe landing. Endurance was set based on half the flight time of UAVs that tended to take video on farmland. Payload was set to be enough to hold a high resolution camera. Span was set to create a large enough platform to easily be able to allow for the payload. Turn Radius was determined based on how much the UAV would need to turn to stay within a 10% buffer on an area the size of an average farm in the US as can be seen in Figure 1.

Endurance was not met and Turn Radius was exceeded. The actual performance of the aircraft will be discussed later.

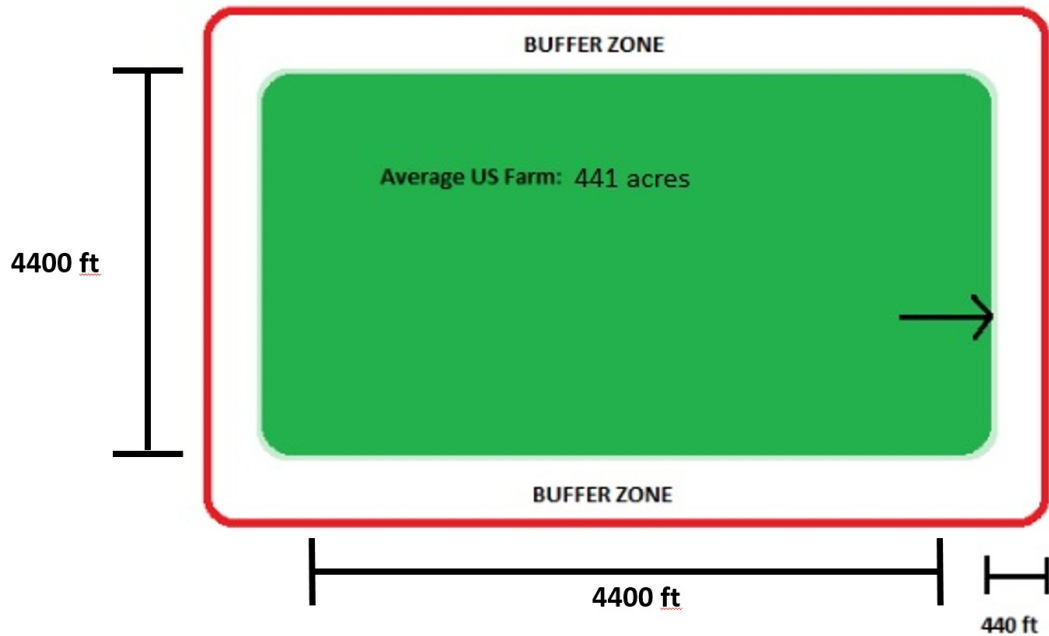


Figure 1: This is an image of a 10% buffer zone around the average area of a US farm and shows how the turn radius was determined.

2.2 Conceptual Design of Aircraft

Due to the inherent instability of a flying wing, an emphasis was placed on stability from the beginning. The airfoil selected is the LA2573A reflexed camber airfoil, designed by Robert Liebeck, head of the blended-wing-body department at Boeing [1]. The airfoil was selected due to its positive moment coefficient, which is a necessary condition for stability in a tailless aircraft. This airfoil also benefits from low drag through a large range of angles of attack, and a lift-curve slope that is standard and predictable. This airfoil also has been used previously in flying wing aircraft such as the NASA AeroVironment Pathfinder and Pathfinder Plus [2]. These aircraft are stable flying wings that also have great endurance characteristics.

The airfoil was analyzed using Airfoil Tools [3], and from that it was determined that in order to obtain the desired performance of this airfoil, a higher Reynolds number was needed. It was decided to shoot for a Reynolds number of 400,000.

This derived requirement was the basic driving force behind much of the rest of the design. In order to obtain the Reynolds number, it was found that a cruise velocity of 40 mph and a chord length of 1 foot was a good balance between velocity and size of the aircraft. In order to produce an adequate amount of lift, a wingspan of 6 feet was chosen. This gave an aspect ratio of 6 and a lifting surface area of 6 square feet. Winglets were deemed necessary in order to have directional stability normally provided by a vertical tail. They were sized comparatively to similar commercial flying wings and confirmed using AVL. From airfoil tools, the expected airfoil characteristics were derived from Figures 3 to 6 and shown in Table 2.

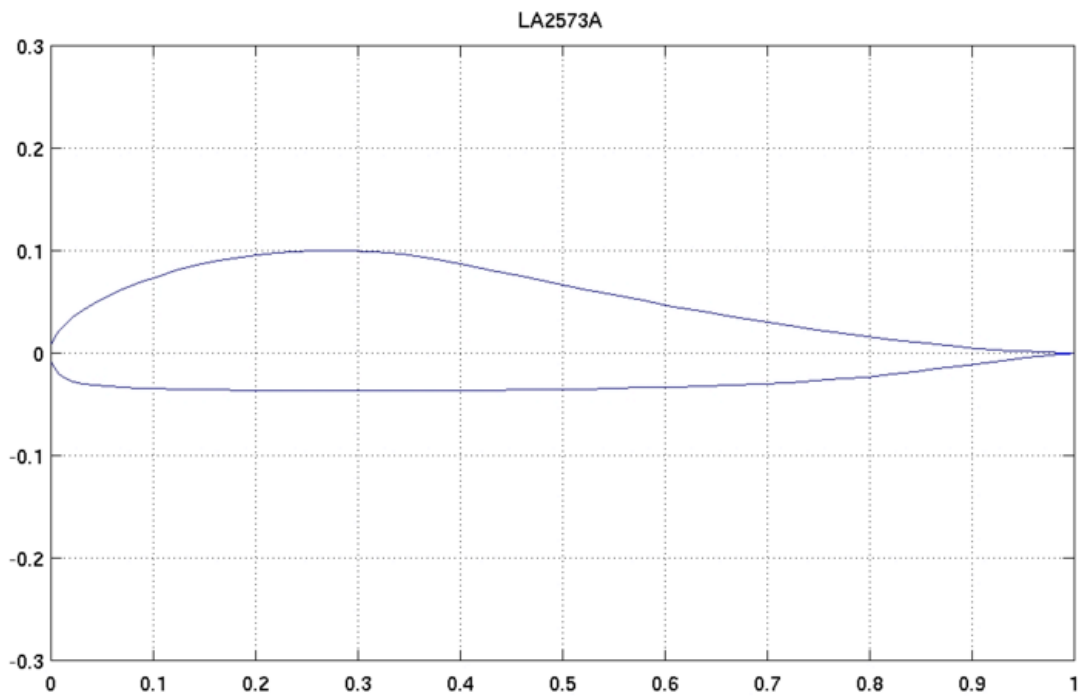


Figure 2: A cross-sectional view of the LA2573A airfoil, showing the slight reflex at the trailing edge.

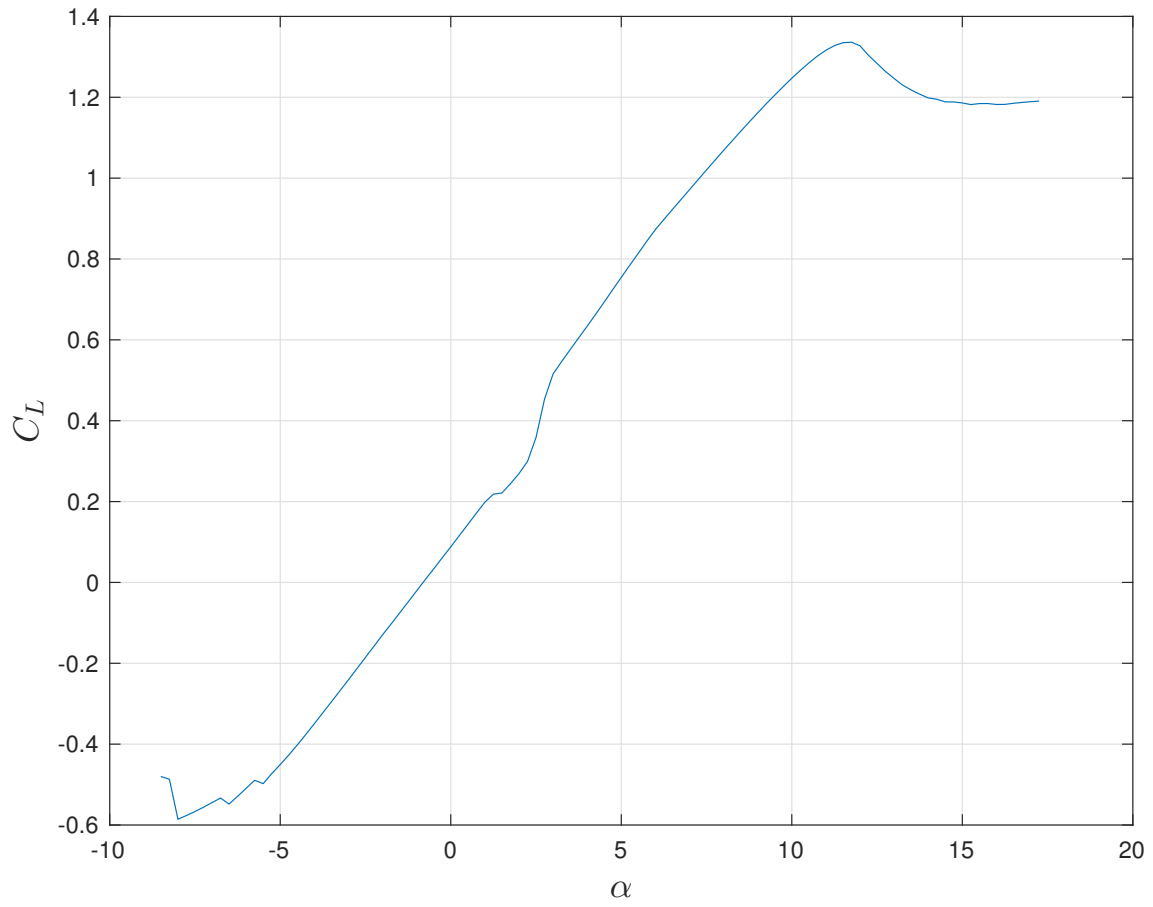


Figure 3: C_L vs α at $R_e = 500,000$ [3]

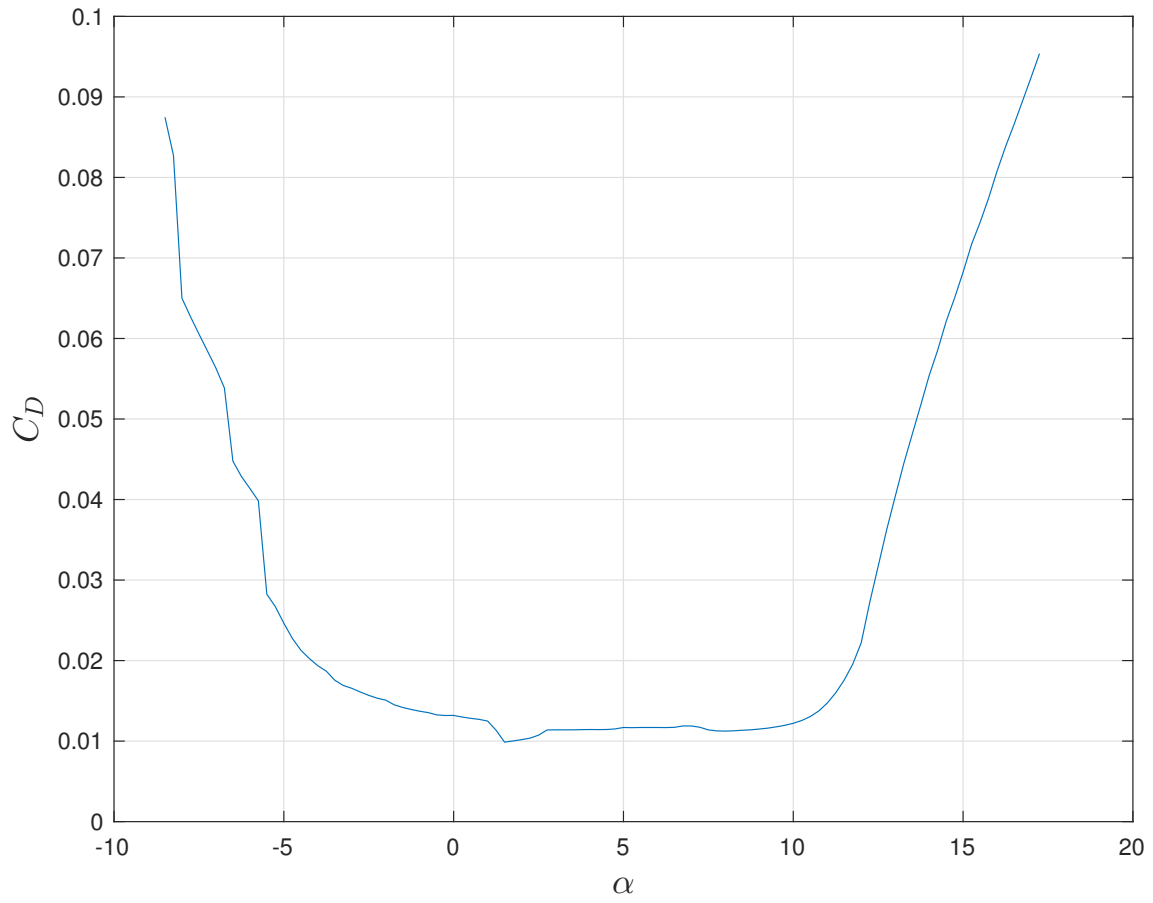


Figure 4: C_D vs α at $R_e = 500,000$ [3]

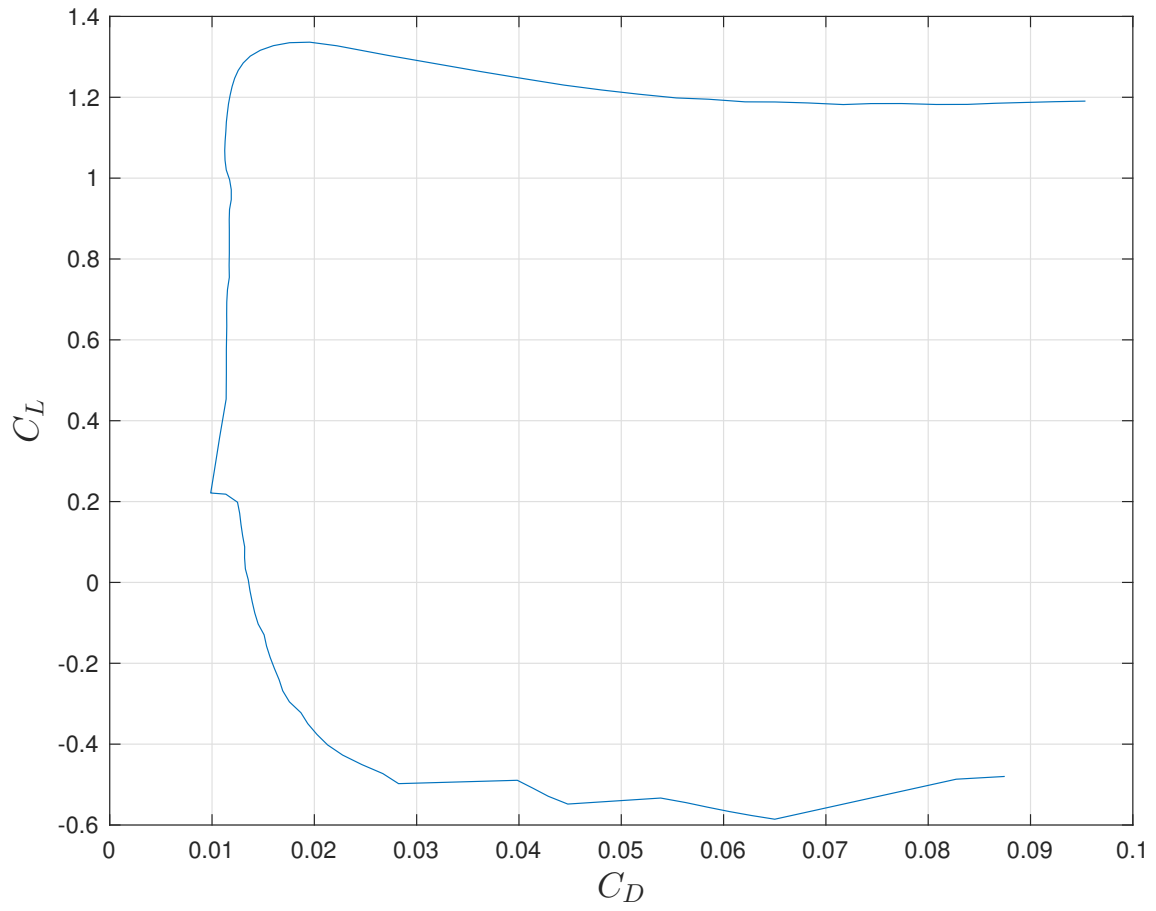


Figure 5: C_L vs C_D at $Re = 500,000$ [3]

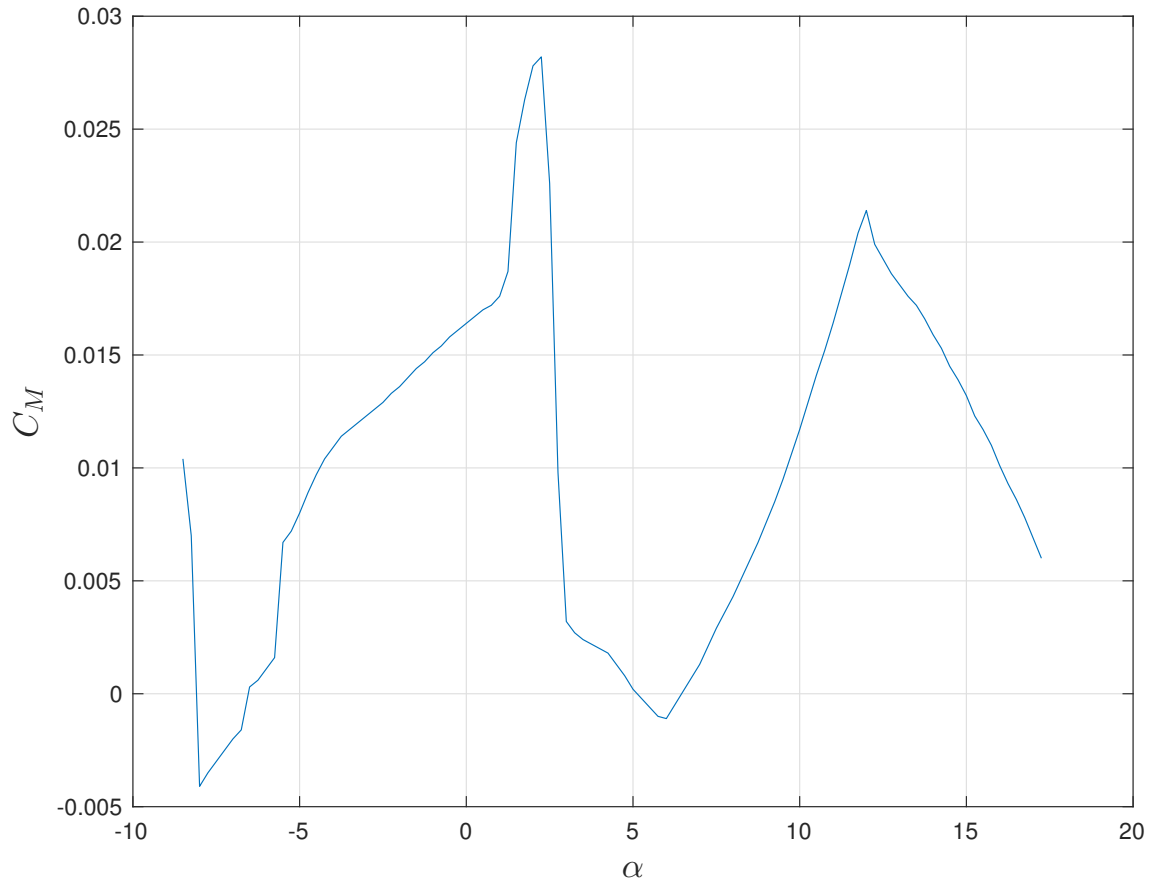


Figure 6: C_M vs α at $R_e = 500,000$ [3]

Aerodynamic Property	Approximate Value
Lift Curve Slope	0.16
Drag Coefficient	0.01
Stall Angle	11°
Pitching Moment	Range: [0.00,0.02]

Table 2: Table of aerodynamic properties for the LA2573A

After looking at other flying wing designs, it was decided that a sweep angle of 15° would benefit the stability of the aircraft for a couple of reasons. The first was due to the need for the coupling of the pitch and roll control of the elevon in the case of a control surface failure. Second, the sweep increases the moment arm that the winglets were able to act on, giving directional stability. This design was modeled in SolidWorks, and the design can be seen in Figures 7 through 10.

For calculating the structural properties the wings several assumptions were made:

1. The wing is under tensile stress only
2. All the force action on the wings was only acting on the carbon tubes and no structural support was being provided by the foam.
3. The carbon tube in the wing acted like a cantilever beam
4. During flight it was assumed that lift was evenly distributed along the wing
5. For calculating the load factor it was assumed all the force was applied to the tip of the wing

To calculate the tensile stress expect the following equations were used:

$$\sigma = \frac{My}{I_x} \quad (1)$$

$$I_x = \frac{\pi}{64}(d_2^4 - d_1^4) \quad (2)$$

$$y = \frac{d_2 + d_1}{2} \quad (3)$$

where σ is the tensile stress, M is the moment being generated on the wing, I_x is the moment of inertia, d_2 is the outer diameter of the carbon tube, d_1 is the inner diameter of the tube, and y is the location where the max stress will occur. To estimate the max wingtip deflection from lift during flight the following equations were used:

$$q = \frac{L}{2b} \quad (4)$$

$$M_{Lift} = \frac{1}{2}qL^2 \quad (5)$$

$$\delta_{tip} = \frac{ql^4}{8EI_x} \quad (6)$$

where q is the distributed load from lift and then divided by 2 so only one wing is considered, L is the lift acting on the wing, b is the span of both wings, M_{Lift} is the moment being generated from lift, E is the elasticity modulus of the carbon tube, l is the length of the wing, and δ_{tip} is the deflection of the wing tip. The tip deflection is calculated to be 0.1 inches meaning it is not a concern and is listed in Table 3. To estimate the max load factor on each wing the following equations was used

$$n_{max} = \frac{\sigma_y I_x}{W_y l} \quad (7)$$

where n is the load factor and W is the weight of the UAV. The max load factor was calculated to be 4.63 meaning that if the UAV was held by the Wing tips you could add 8 time the weight of the UAV in the middle before the wings were fractured. This value is listed in Table 3

Structural Property	Approximate Value	Interpretation
Max Tip Deflection	0.1 inches	Flutter is not a concern
Max wing Load factor for one wing	4.63	With both wings the Load factor is over 9 which is structurally sufficient

Table 3: Table of wing load properties

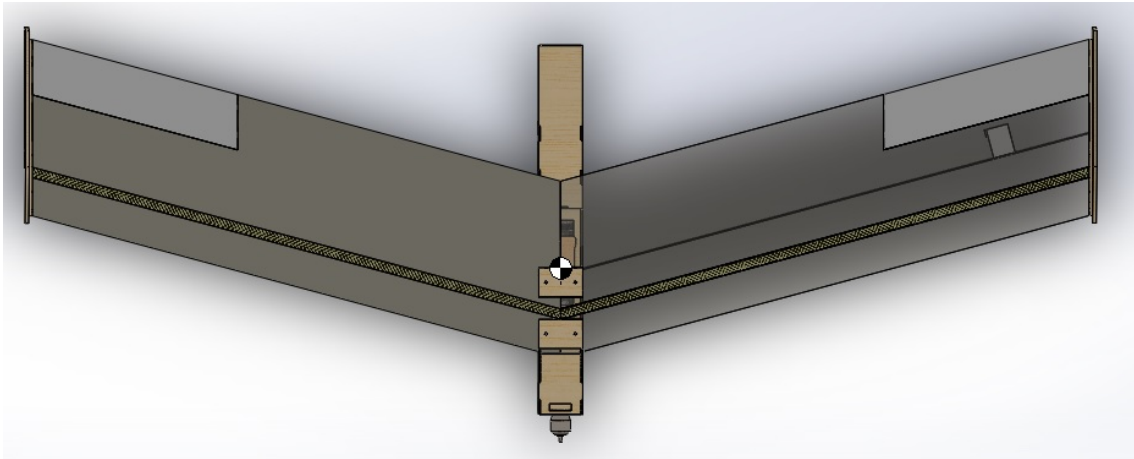


Figure 7: Top view of the SolidWorks model of the UAV. The solid line going through both wings is the carbon rod support for the structure. The line running through the port wing is showing where the carbon spar was placed to add stiffness to the wing. The light grey box flush with the carbon spar is the location for the servo placement.

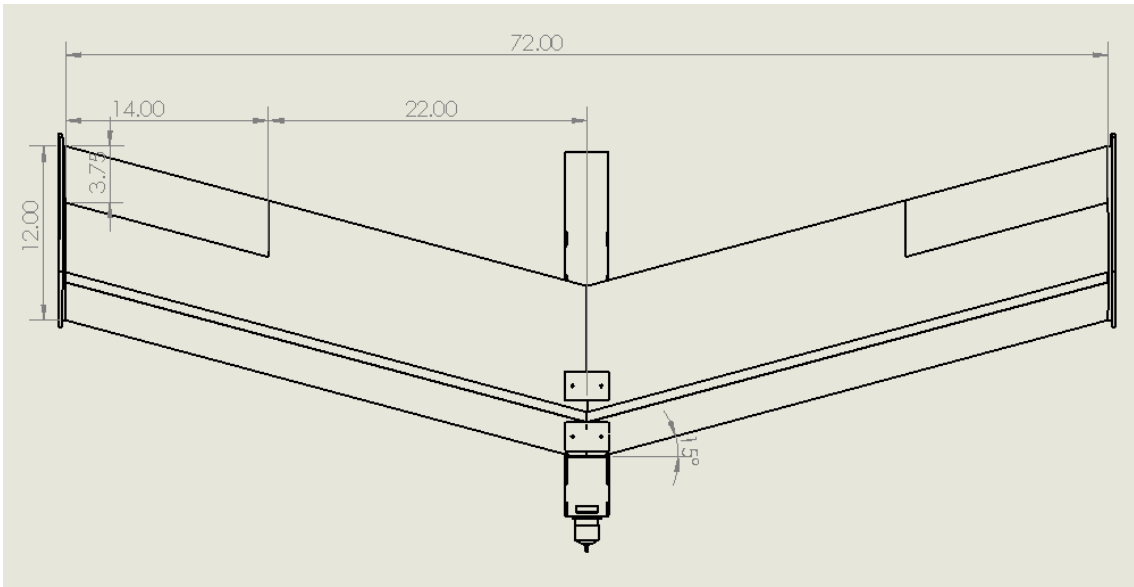


Figure 8: Top view of the SolidWorks drawing of the UAV with dimensions. All units are in inches.

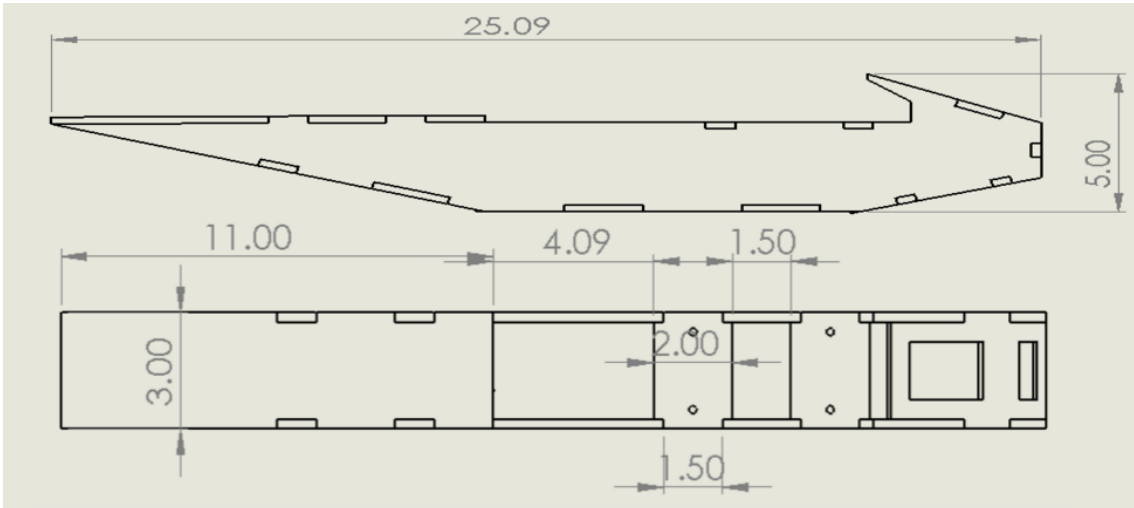


Figure 9: SolidWorks drawing of the fuselage with dimensions. All units are in inches.

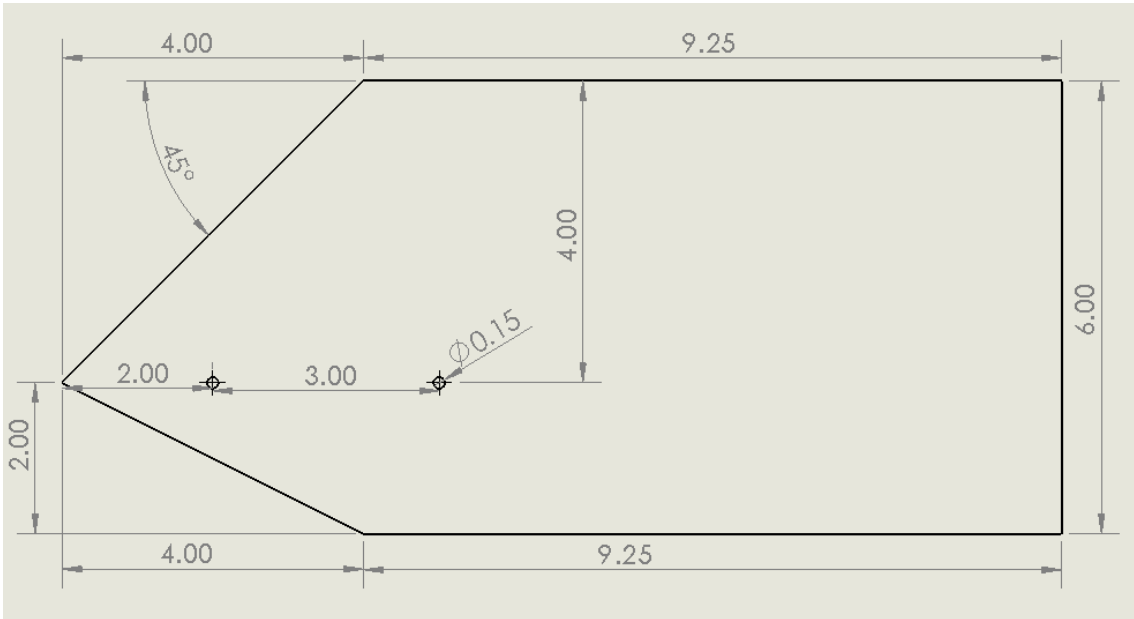


Figure 10: SolidWorks drawing of the winglet. All units are in inches.

2.3 Performance Analysis

After the initial design decisions, very basic and preliminary calculations were done to verify that the design would indeed be feasible. First, cruise conditions were calculated by assuming a total weight of 5 pounds. At cruise, the lift generated by the wings can be equal to the weight. Given these conditions, the following equation holds true.

$$C_L = \frac{2W}{\rho V^2 S} \quad (8)$$

Also, assuming a cruise velocity of 40 mph, it can be deduced that for a surface area of 6 square feet, a lift coefficient of 0.20 is necessary for equilibrium. According to the airfoil polars taken from Airfoil Tools shown in Figure 2, this also yields an angle of attack at cruise of approximately 1° . At the given lift value, the drag coefficient will be approximately 0.15. This calculation was used to verify that the selected lifting surface area was appropriate given the expected weight and cruise velocity of the aircraft.

The maximum lift to drag ratio was calculated using

$$\left(\frac{L}{D}\right)_{max} = \frac{1}{2} \sqrt{\frac{\pi AR \epsilon}{C_{D_o}}} \quad (9)$$

Assuming a span efficiency factor of $\epsilon = 1$, the maximum lift to drag ratio for this aircraft is 17.72.

The performance analysis related to battery, motor, and propeller selection will be presented in Section 3.2. Additionally, analysis of the control surfaces will be presented in Section 2.4.

2.4 Control Surface Sizing and Placement

Designing the control surfaces of the aircraft was a challenge that required many different approaches. The final approach that was taken was using AVL software that utilizes the vortex-lattice method (Figure 11). By changing the size of the control surface in the software iteratively, the ideal design was able to be achieved. The goal was to reach an effective one to one ratio between pitch and roll moments for a given control surface deflection. It was discovered that the smaller the control surface and the farther out along the wing, the closer the pitch and roll moments were to being equal. A limit was set using a volume coefficient set by other similar sized aircraft. Another factor of the pitch to roll moment ratio is the placement of the center of gravity. The volume coefficient that was used was 0.126. Using this volume coefficient, the control surface was sized to be 14 inches in span, 31.25% of the chord, placed all the way at the tips of the wings, and cut out of the wing. This gives a pitch to roll moment ratio of 1.28 when the center of gravity is placed 0.25 inches in front of the neutral point. From AVL, the neutral point was given to be about 7 inches from the leading edge of the middle of the wing, so the center of gravity was placed at 6.75 inches from the leading edge of the middle of the wing. See the figure below for stability derivatives.

```

-----
Vortex Lattice Output -- Total Forces

Configuration: Single Control Surface UAV
# Surfaces = 3
# Strips = 112
# Vortices =1792

Sref = 864.00      Cref = 12.000      Bref = 72.000
Xref = 7.5000     Yref = 0.0000      Zref = 0.0000

Standard axis orientation, X fwd, Z down

Run case: -unnamed-

Alpha = 0.00000   pb/2V = -0.00000   p'b/2V = -0.00000
Beta  = 0.00000   qc/2V = 0.00000   r'b/2V = -0.00000
Mach  = 0.000     rb/2V = -0.00000

CXtot = -0.05016  Cltot = 0.00000    Cl'tot = 0.00000
CYtot = -0.00001  Cmtot = 0.02360
CZtot = -0.02130  Cntot = 0.00001    Cn'tot = 0.00001

CLtot = 0.02130  CDtot = 0.05016
CDuis = 0.05000  CDind = 0.00016
CLff  = 0.02120  CDff  = 0.00002   | Trefftz
CYff  = -0.00000   e    = 1.0455    | Plane

Lelevon = 0.00000
Relevon  = 0.00000

-----

Stability-axis derivatives...

                alpha                beta
-----
z' force CL | CLa = 4.451866   CLb = -0.000000
y force CY | CYa = -0.000123   CYb = -0.186420
x' mom. Cl' | CLa = 0.000013   CLb = -0.039665
y mom. Cm | Cma = -0.012609   Cmb = 0.000000
z' mom. Cn' | Cna = -0.000135   Cnb = 0.010198

                roll rate p'          pitch rate q'          yaw rate r'
-----
z' force CL | CLp = 0.000001   CLq = 4.443298   CLR = -0.000000
y force CY | Cyp = -0.054876   CYq = -0.000074   CYr = 0.049885
x' mom. Cl' | Clp = -0.527235   Clq = 0.000000   Clr = 0.015717
y mom. Cm | Cmp = 0.000001   Cmq = -1.056085   Cmr = -0.000000
z' mom. Cn' | Cnp = 0.002117   Cnq = 0.000083   Cnr = -0.005098

                Lelevon d1          Relevon d2
-----
z' force CL | CLd1 = 0.008070   CLd2 = 0.008070
y force CY | CYd1 = 0.000403   CYd2 = -0.000403
x' mom. Cl' | Cl d1 = 0.002709   Cl d2 = -0.002709
y mom. Cm | Cmd1 = -0.003472   Cmd2 = -0.003472
z' mom. Cn' | Cnd1 = -0.000091   Cnd2 = 0.000092
Trefftz drag | CDffd1 = 0.000011   CDffd2 = 0.000011
span eff. | ed1 = 0.270001   ed2 = 0.269987

Neutral point Xnp = 7.034230

Clb Cnr / Clr Cnb = 1.261613 ( > 1 if spirally stable )

Operation of run case 1/1: -unnamed-
=====

```

Figure 11: Stability derivatives calculated on AVL.

3 Build

3.1 Build Readiness Review

The motor was initially chosen to be an E-flite Power 10 with a 14x8 Prop but was determined to be far more powerful than necessary at the Build Ready Review. The initial motor had a climb rate of 3000 ft/s which was far higher than the desired 1300 ft/s. The motor, propeller, and battery were sized down to the E-flite Power 32 with a 10x8 Prop; the details will be given later.

Initially there was some concern about the winglet sizing because of its importance for lateral stability. The calculations were later checked on AVL and were confirmed to provide enough stability for the aircraft. The winglets were then designed to be taller on the top than on the bottom so there would be clearance between the winglet and the ground on landing.

During the build readiness review there was some concern over the initial sizing of the control surface. The surface was only 6.95 inches in span with a chord of 2.5 inches, making it a third of the area of what the final control surface was. The control surface was also not placed at the wing tips, but was instead located about two thirds of the way down the wing. The main concern was that the control surface was too small and would not have the effectiveness to control the aircraft. After the build readiness review is when AVL was used to assist in sizing the control surface and provided much better results.

3.2 Component Selection and Sizing

The motor was sized using the online motor calculator eCalc [5] and Matlab to find dynamic thrust and climb rate. A desirable rate of climb was decided to be 1300 ft/min around takeoff velocity and all motor prop combinations were sized to reach this amount. Taking the static thrust and pitch velocity from eCalc's database of motor prop combinations the climb rate vs velocity can be found and the desired climb rate can be acquired using the following equations,

$$\begin{cases} \frac{P}{D} \leq 0.6 : T_{dyn} = T_{stat} \left(1 - \frac{V}{V_{pitch}} \left(\frac{\frac{P}{D}}{\frac{P}{D} + 0.2} \right) \right) \\ \frac{P}{D} \geq 0.6 : T_{dyn} = T_{stat} \left(1 - 1.25 \left(\frac{V}{V_{pitch}} \frac{1}{\frac{P}{D}} - \left(\frac{P}{D} - 0.6 \right) \right) \right) \\ T_{dyn} > T_{stat} : T_{dyn} = T_{stat} \end{cases} \quad (10)$$

$$V_{pitch} = \Omega P \quad (11)$$

Where P is prop pitch, D is prop diameter, T_{dyn} is dynamic thrust, T_{stat} is static thrust, V is velocity and Ω is rotational speed of the prop. The motor prop combination was found to give a high enough pitch speed to maintain speeds 1.5 times higher than cruise while also giving an acceptable rate of climb at takeoff.

The battery was chosen to be a 3200mAh 4s 14.8V 30C Li-Po Kinexsis Battery. The 3200 mAh gives the plane approximately 10 minutes of flight time, which was determined to be enough for test

flights while not adding too much weight as to make flight difficult. Increasing the mAh linearly increases the weight of the battery as more parallel cells are added, increasing mAh instead of the voltage increase from cells in series. The 4s rating on the battery is from 4 cells being wired in series giving the 14.8V to the battery. Increasing the voltage of the battery increases the rotational speed of the motor while causing higher heat in the motor, causing the tradeoff to be between a motor's ability to handle heat and the desired rotational speed. The 30C rating is the discharge rate of the battery and is of lesser importance, as higher discharge rates are only necessary for platforms that require a lot of power very quickly such as a quadcopter.

The Electronic Speed Controller (ESC) was chosen to be an E-Flite 40A brushless ESC to match the E-Flite Motor. The motor was given to never draw more than 31A by eCalc and so giving a large safety factor, a 40A ESC was chosen so that the ESC's limit would never be reached by the current draw.

When picking a motor prop combination, to quickly find desirable rate of climb characteristics the power required for that rate of climb should first be found. A motor should be picked from that required power and then a prop should be picked to match that motor. High diameter low pitch props give high rate of climb and low maximum speed as the high diameter provides powerful thrust but the low pitch gives small pitch speed which leads to lower dynamic thrust at higher speeds. Low diameter high pitch props give low rate of climb and higher maximum speed as the low diameter gives less thrust but the high pitch gives a high pitch speed which leads to higher dynamic thrust at higher speeds. Using an online calculator like eCalc to test the current draw and static thrust of the combinations desirable characteristics can be found. If the motor current draw is too far below maximum, then the motor will not run at peak efficiency and a smaller motor should be chosen. If the current draw is too high then a larger motor should be chosen, and the process repeated.

Refer to Figure 12 to see the climb rate vs velocity of the E-Flite Power 32 Motor with the 10x8 folding prop. Multiple motor prop combinations were tested from the E-Flite Power series of motors and this combination was found to be the most effective.

In addition to the propulsion system components, we decided to go with an avionics package in order to both accurately record the flight data as well as simulate a failed control surface at the command of a switch on the ground. The Pixhawk unit, sold by 3D Robotics (3DR), was selected due to its ease of use, and its ability to be modified and customized. Additionally, 3DR and other aftermarket vendors sell easily compatible sensor packages. In addition to the Pixhawk flight computer, the Pixhawk GPS/Magnetometer module, digital airspeed sensor, and 915 MHz telemetry radios were purchased. It was confirmed through email with a 3DR representative that both the airspeed sensor and telemetry radios were discontinued by 3DR. These components were purchased through other sources.

The firmware used on the Pixhawk module was the open source PX4 Flight Stack software from Pixhawk [4]. The ground station software used to calibrate, initialize, record data, and monitor flights was the QGroundControl. This program was found to be less buggy than other commonly used programs, especially with regards to calibration of the various sensors. Within QGroundControl, there are many choices for the type of airframe that could be used. However, we had to create a custom airframe to enable the full range of our servos. The servo rail on the Pixhawk is configured so that the ESC, which powers the servo rail, is plugged into Pin 4. The left and right elevons are

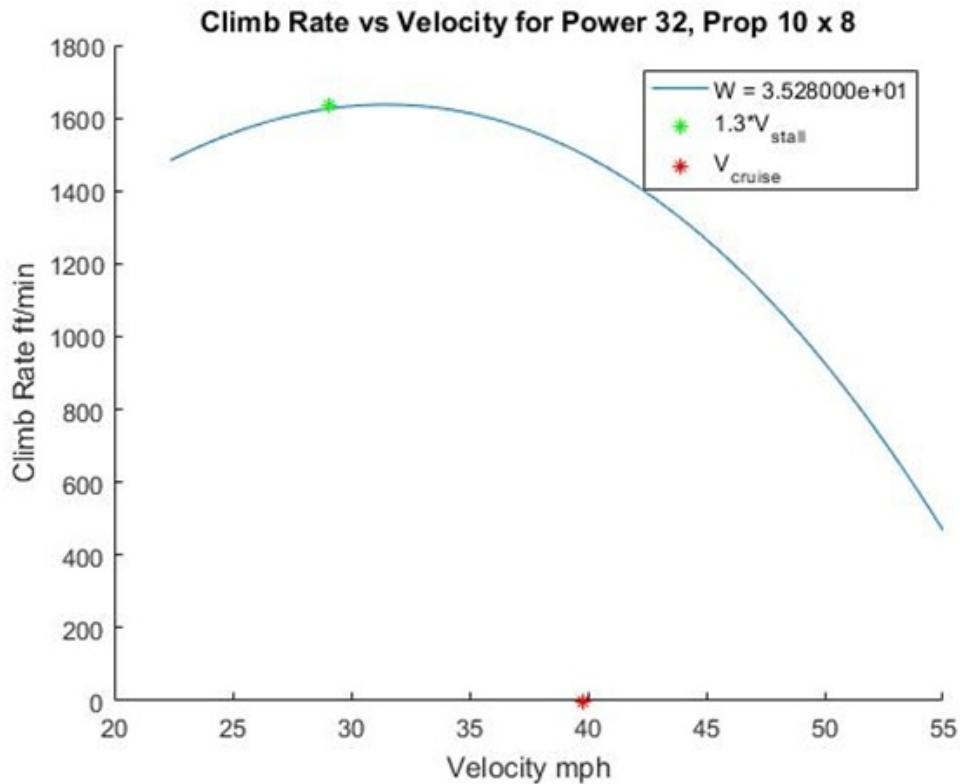


Figure 12: This is a climb rate vs velocity graph for the E-Flite Power 32 motor with a 10x8 folding prop. The $1.3V_{stall}$ is the expected take off speed and the V_{cruise} is the expected cruise speed. This graph shows that the motor is capable of moving the UAV at a speed higher than cruise as well as having a desirable climb rate at takeoff of >1300 ft/min.

plugged into Pins 1 and 2. It does not matter which elevon is plugged where, as their signals can be flipped within the QGroundControl parameter controls. Both the magnetometer wires as well as the digital airspeed sensor wires need to be connected to the i2c splitter module, which is then in turn connected directly to the Pixhawk.

The servos were selected for their combination of small size and large torque capabilities. The small size was deemed important due to the very slim profile of the airfoil and so it could be embedded in the foam without compromising the aerodynamics of the airfoil. The torque produced by the servos was also important to consider, due to the high flight speeds that the aircraft was expected to reach. After looking at many different options, the 125MG Micro Thin Wing Servo from Hitec was selected. It has a thickness of 0.39 inches and produces 49 oz.-in of torque, which far exceeds the estimated required torque of 18 oz.-in.

3.3 Build Details

The fuselage was constructed by laser cutting all pieces from a sheet of 5-ply aircraft grade birch wood. All of the pieces except for fuselage front and the fuselage back top were glued together using wood glue and clamps to apply pressure and keep pieces locked in place. The fuselage back top was left unglued in order to access that section when dealing with the telemetry antenna. During flight, tape is applied to keep the piece on (Figure 13). Tee nuts were applied to the fuselage wing attach pieces for the wing to be able to bolt into (Figure 14). Before gluing the fuselage front on, tee nuts were put in for the motor to screw into. Divots were cut into the fuselage front as well so the motor could sit flush. After a few flights, it was found that the thrust line was off when the motor was flush, and washers were added to the top bolts in order to tilt the motor down (Figure 15). In order to apply more gluing area for the fuselage front, six triangular gussets were added and glued in at the same time as the fuselage front. CA glue was applied after the wood glue had set to provide more reinforcement.



Figure 13: View of the back of the fuselage. The black tape is holding down the top plate and a hole was cut in the bottom for airflow.

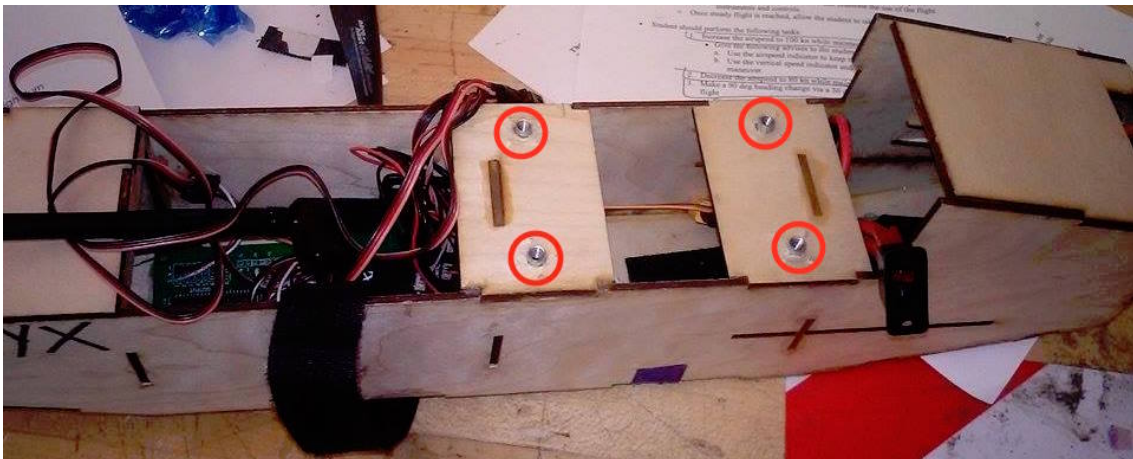


Figure 14: View of the top of the fuselage without the wings being attached. The velcro strap was used to help secure the battery inside the fuselage. The two plates going across the main body is where the wings were screwed into (with the Tee nuts circled)



Figure 15: View of the motor attached to the front of the fuselage. Washers were added to the top bolts (circled in red) to tilt the motor down in order to align the thrust line to be parallel with the fuselage.

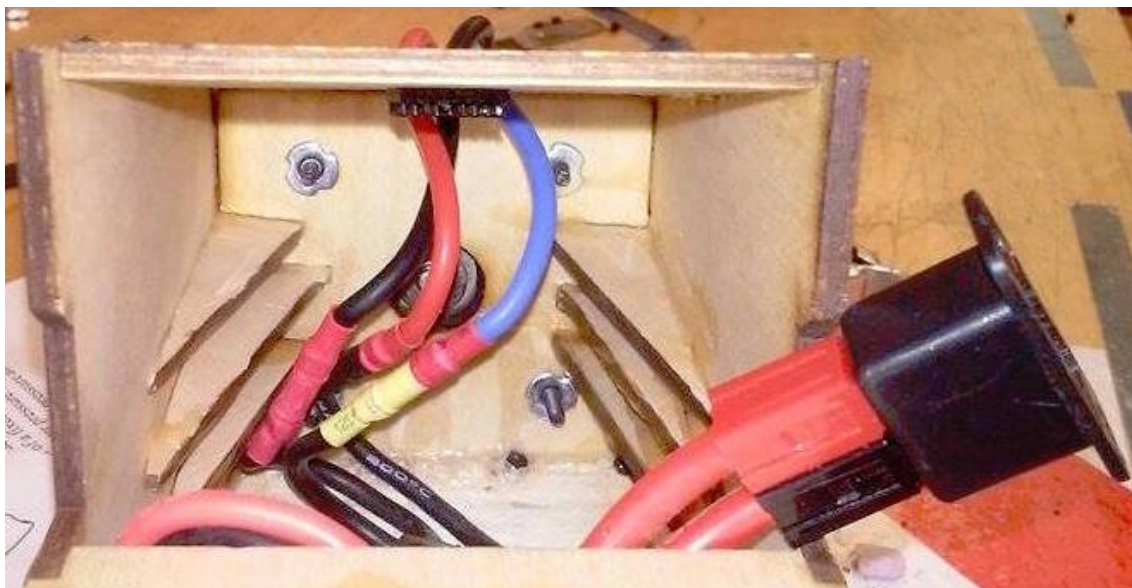


Figure 16: Inside view of the front of the fuselage where the motor is attached to. The black and red cable on the right is the connection for the shunt. The triangular wooden pieces are the gussets to had structural support to the front plate. The blue, red, and black wires in the middle connect the motor to the ESC.

The wing was constructed from foam. The foam core used for the wing arrived as two sections, each a straight wing with a length of 90 inches. The first step was to cut each section, using a hot wire, to be swept back 15 degrees as well as 36 inches in length span wise. This resulted in the wing having an actual length of 37.27 inches as measured along the leading edge. With the planform of the wing being done, a channel was cut out of each section for the carbon fiber tube (Figure 17). The channel was cut out using a router that had an edge guide. The carbon fiber tube was glued in using 30 minute epoxy at the same time that the wings were glued together at the center. With the wings glued together, the router was used to level sections of the center of the wing for the wing attach support pieces to be glued to. Due to difficulties of lining the pieces up, they were actually put on slightly crooked. In order for the wing to still be able to be screwed down to the fuselage, the holes were drilled to be slightly larger so they could rotate and still have all four bolts fit through the holes (Figure 18). The final wood pieces that were added to the wing were the winglet and the winglet attach pieces (Figure 19). The winglet attach piece was glued to each end of the wing after threading the two holes for the #10-32 nylon screws. Initially the winglets were also threaded and a headless screw was used. After some advising from others, the threads were drilled out and nylon bolts with heads were used to hold the winglets on. Next, the carbon fiber support spar was added to the bottom of each half of the wing. A slot was cut out using a knife and the spar was pressed in. Then epoxy was applied across the top and within any gaps.



Figure 17: View of the port side foam wing with the channel cut out for the carbon spar.

The control surfaces of the wing were cut out by measuring along the trailing edge and along the chord and using a knife to cut. The control surfaces were attached to the wing using a thin piece of balsa glued to the control surface and the wing, and then screwing nylon hinges into the balsa (Figure 20). For extra support, the hinges were also glued down. The actuators were attached by using the router to cut a section out of the bottom of the wing. The section was cut deep enough for the actuator to sit flush with the bottom of the wing. A piece of wood was glued into the cutout and the actuators were screwed into the wood. A control horn was glued to the control surface after lining it up with the control arm coming off the actuator (Figure 21). A push rod was then attached to the control arm and control horn and adjusted until the control surface was deflected up a few degrees when in the neutral position.

The next step for finishing the wing was cutting the channels for all the wires. This was done just

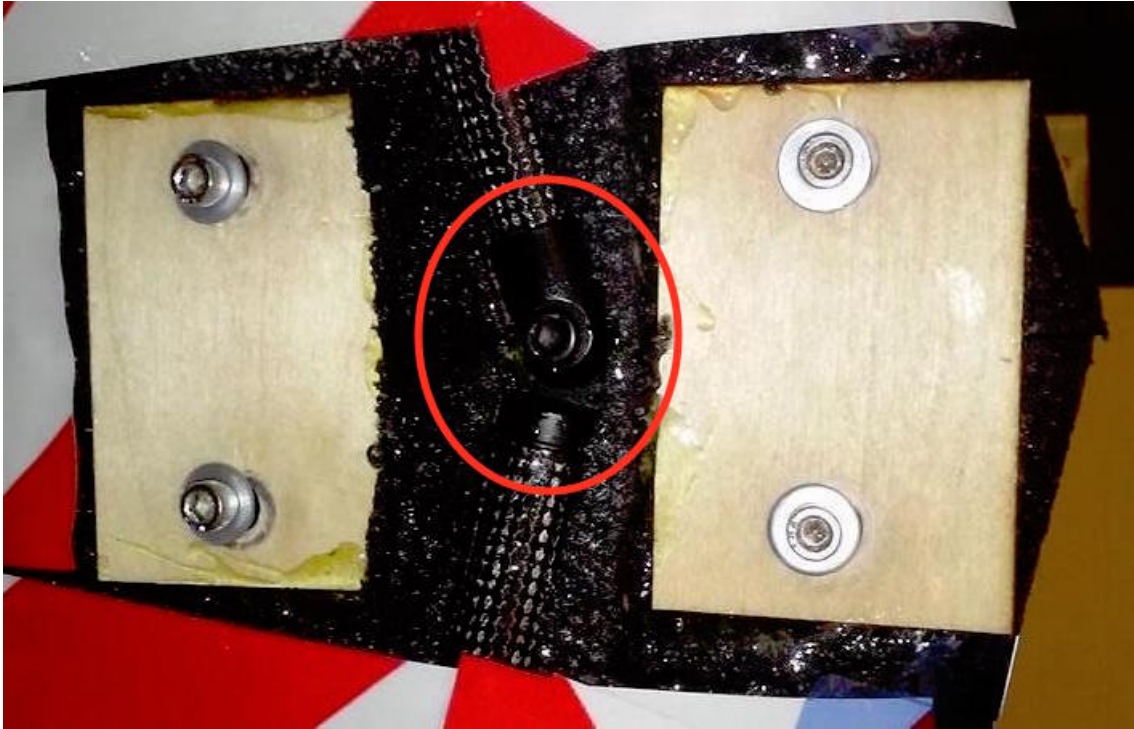


Figure 18: View of the wing connection and bolts used to connect the wing to the fuselage with the leading edge on the right and the trailing edge on the left. You can see the aluminum connector in the middle attaching the carbon rods of both the wings.

using a pair of pliers and pulling the foam out bit by bit. This was done for the servo wires and the pitot tube. The pitot tube was attached using two wood pieces with holes cut out for a carbon fiber tube to fit in (Figure 22). The pitot tube was glued to the end of the carbon fiber tube and the wood pieces were glued into the wing using 5 minute epoxy. 5 minute epoxy was used so that if the pitot tube hits the ground, it would easily pop off the wing. The pitot tube was initially glued to the bottom of the wing, but after coming off in flight, it was placed on the top of the wing. The final step for completing the wings was to add a skin. A red and white polyethylene barricade tape was used to cover the top of the wing, and 3M 8951 polyester tape was used to tape the bottom (Figure 23). Then CA glue was applied to the edges to ensure the skin would not come off during flight.

The final portion of the build was placing the avionics within the aircraft. In order to make removal of the wing as simple as possible, the two actuator connections, the GPS connection, and the i2c splitter connection were combined into one connection. The magnetometer off the GPS and the pitot tube went through the i2c splitter. The rest of the avionics were placed into the fuselage with the pixhawk on top of the battery and then strapped down so they would not move during flight. The position of the battery was the main component of balancing the center of gravity.



Figure 19: View of the port side winglet with the nylon bolts attaching it to the wing.



Figure 20: View of the starboard wing end and elevon. A counter weight is taped onto the winglet to balance out the pitot tube on the port side wing. In the blue circle the hinges for the elevons are shown screwed and glued into pieces of wood attached to the elevon and the wing.



Figure 21: View of the bottom of the port side wing and elevon. Below the control arm (circled in red) is the carbon spar inserted into the elevon to give it some rigidity. To the left of the servo is the connection wires imbedded in a channel pulled out using plier and covered in tape.



Figure 22: View of the pitot tube on the port wing. A carbon tube holds the pitot tube out in front of the leading edge and away from the motor to get the most accurate reading.



Figure 23: View of the starboard wing from the leading edge showing the skin contrast between the top and bottom of the wing. The bottom is a clear blue and the top is a bright red and white stripe.

3.4 Final Weight and Moment of Inertial Swings

The final weight of all necessary components of the aircraft was 5.5 pounds. An additional 0.5 pounds of "payload" was added to the aircraft to balance the wings and place the center of gravity 0.25 inches in front of the neutral point of the wing.

The moments of inertia were found using a compound pendulum test for pitch and roll, and a bifilar test for yaw. The moment of inertia of the frame and rig are both known and subtracted from the final calculated moment of inertia. The moment of inertia for pitch is $2.58 \text{ lb} \cdot \text{ft}^2$. The moment of inertia for roll is $9.42 \text{ lb} \cdot \text{ft}^2$. The moment of inertia for yaw is $11.31 \text{ lb} \cdot \text{ft}^2$. Below are images of all three test set ups.

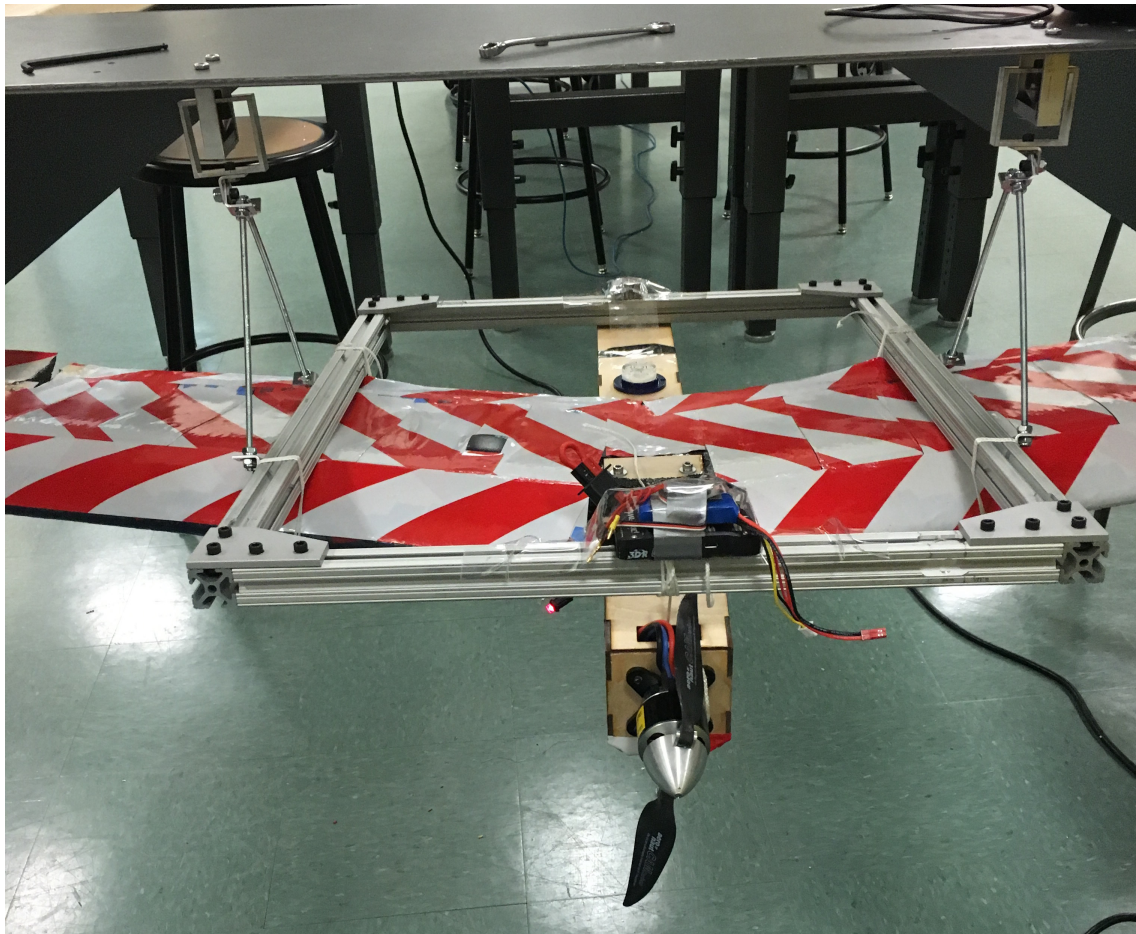


Figure 24: This figure shows the aircraft in the pitch compound test set up.

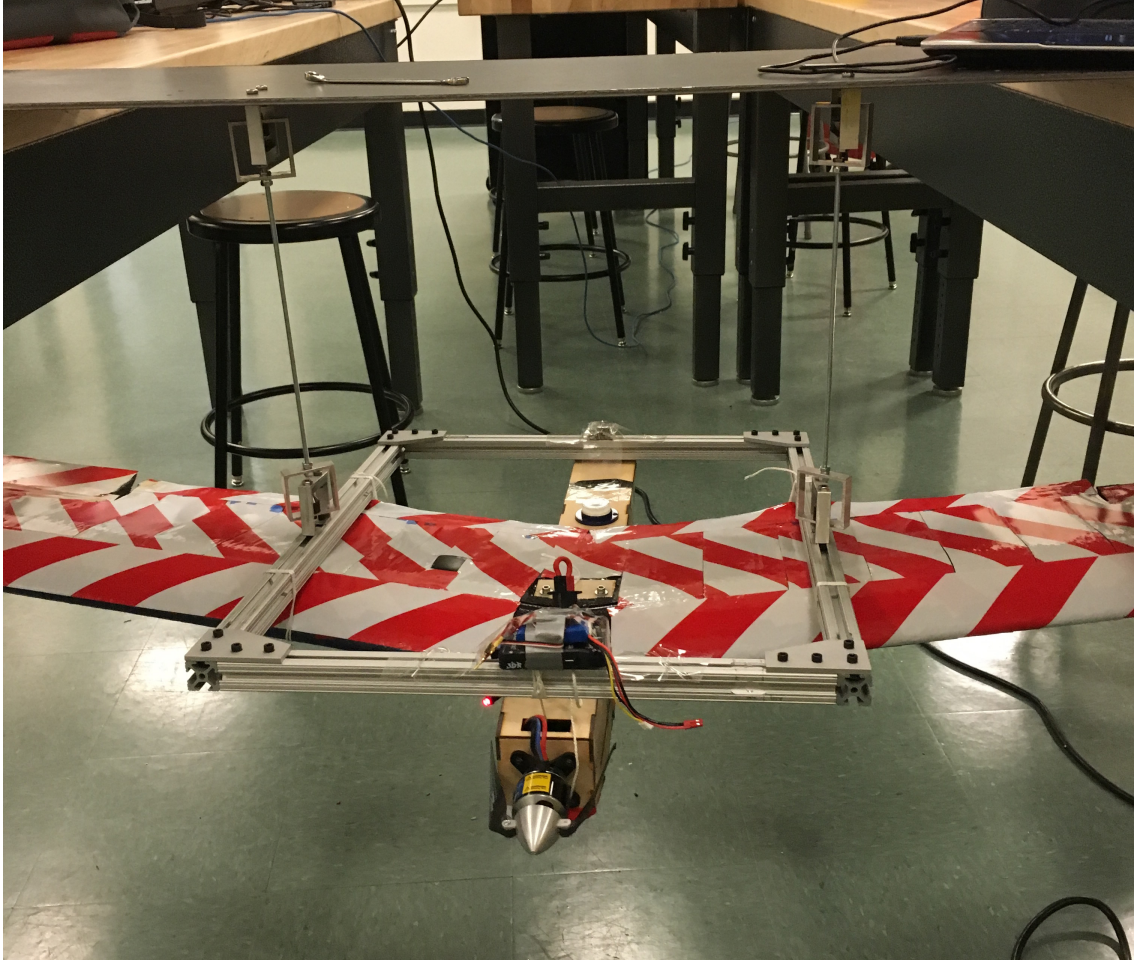


Figure 26: This figure shows the aircraft in the yaw bifilar test set up.

4 Flight

4.1 Flight Readiness Review

For the flight readiness review the UAV build was all finished except for the skin which had not been put on yet. The controller was paired to the UAV and the control surfaces and motor were operational.

To start, the pilot (Curtis Olson) went over the entire aircraft to spot any corrections that needed to be made. It was requested from the pilot that the top of the wing have a different brighter color than the bottom, as seen in Figure 23, to make it easier to see the UAV's orientation while flying.

When testing the lateral balance of the UAV it was found that the port side was heavier than the starboard side due to the pitot tube being attached to the port wing. To compensate we attached a small counter weight to the starboard winglet (Figure 20).

Between the elevons and the wings there was a gap where the hinge was connecting the two together. Left alone this gap would have cost a loss of effectiveness in the elevon when flying from the airflow leakage through the gap. As seen in Figure 20 this was solved by taping over the gap with the same tape used for the top skin of the wings. The pilot also requested the elevons to be deflected up a few degrees in the neutral position. From experience the elevons are need to be deflected up slightly to keep the UAV in trim while flying.

After the look over from the pilot Chris Regan and Brian Taylor from the UAV lab examined our UAV. Their first suggestion was to cut a hole in the back of the fuselage (Figure 13) to allow air to flow through the fuselage to cool the ESC and other electrical components.

Originally the winglets were screwed in with nylon screws with a grub head and were threaded into the winglet and winglet attach on the wing. Chris and Brian recommended using nylon screws with a head and only having the winglet attach be threaded, so that in the event of a crash the nylon screws would take the impact instead of the wing. This would cause the winglets to break off instead of causing damage to the wing in a crash.

When testing the rigidity of the elevons Chris found that they were too 'floppy' because the only structural support they had was the foam they were made out of. This 'floppiness' left uncorrected would reduced the effectiveness of the elevons. To add stiffness, carbon spars were inserted into the elevons the same way the carbon spars were added to the wings which gave some rigidity to the winglets.

The final correction made by Chris and Brian was to set the minimum voltage warning above the ESC shutoff voltage. In our original set up the warning was set to the same voltage as the ESC shutoff rendering the warning to be useless. By setting the voltage higher it allowed us to have time to land the UAV during flight before the ESC would power down which would cut power to the motor and the elevons.

4.2 Pre Flight Checklist (Before Departure)

- Aircraft Physical Check
 1. Airframe has no physical damage
 2. Motor is secure and undamaged
 3. Prop is undamaged and NOT attached
 4. Servos and wires are secured and undamaged
 5. GPS receiver and cable are secured
 6. Telemetry module and cables secured and undamaged
 7. RC receiver and wires are secured and undamaged
 8. Wings unattached
- Ground Station
 1. Laptop(s) turned on and battery lifespan confirmed
 2. Start up Ground Control
- Avionics and Controls
 1. Check that UAV battery is fully charged and attach to bottom of fuselage with Velcro straps
 2. Check that controller battery is fully charged
 3. Make sure SD card has free space and is working
 4. Connect Pixhawk to UAV
 5. Connect Pixhawk to battery (Have shunt out!)
 6. Attach wings
 7. Connect to Ground control
 8. Make sure prop is not connected to motor
 9. Connect shunt

10. Check all calibrations (GPS, telemetry etc.)
 11. Pair controller to Pixhawk
 12. Pitch up (Both elevons up)
 13. Pitch down (Both elevons down)
 14. Roll right (Port elevon down starboard up)
 15. Roll left (Port elevon up starboard down)
 16. Test throttle
- Prepare UAV for departure
 1. Disconnect shunt
 2. Take off the wings
 3. Disconnect battery
 - Tools/Spares to bring
 1. Battery charger
 2. Extra battery(s)
 3. Allen key for wing attachment
 4. Screw driver for motor
 5. Extra screws for winglets
 6. Extra Props
 7. Tape used for skin
 8. FAA card
 9. Camera/Phone
 10. Wing Attach bolts
 11. 5 minute epoxy

4.3 Pre Flight Checklist (On Site)

- Aircraft Physical Check
 1. Airframe has no physical damage
 2. Motor is secure and undamaged
 3. Prop is undamaged and NOT attached
 4. Servos and wires are secured and undamaged
 5. GPS receiver and cable are secured
 6. Telemetry module and cables secured and undamaged
 7. RC receiver and wires are secured and undamaged
 8. Wings unattached
- Ground Station
 1. Laptop(s) turned on and battery lifespan confirmed
 2. Start up Ground Control
- Avionics and Controls
 1. Check that UAV battery is fully charged and attach to bottom of fuselage with Velcro straps
 2. Check that controller battery is fully charged
 3. Make sure SD card has free space and is working
 4. Connect Pixhawk to UAV
 5. Connect Pixhawk to battery (Have shunt out!)
 6. Attach wings
 7. Make sure everyone is behind UAV
 8. Attach prop to motor
 9. Plug in motor

10. Connect to Ground control
 11. Connect shunt
 12. Check all calibrations (GPS, telemetry etc.)
 13. Pair controller to Pixhawk
 14. Pitch up (Both elevons up)
 15. Pitch down (Both elevons down)
 16. Roll right (Port elevon down starboard up)
 17. Roll left (Port elevon up starboard down)
 18. Test throttle to max
- Take off procedure
 1. All team members behind the UAV (excluding launcher)
 2. Point the UAV facing into the wind
 3. 1 team member ready to hand launch UAV (Thrown holding fuselage)
 4. 1 team on computer to relay inflight information to pilot
 5. 3 team members ready to film the flight
 6. Pilot engages the throttle and instructs the team member holding the UAV when to throw it

4.4 Flight Tests

For the first flight the UAV was tested without failing a control surface. The first part of the flight plan was for the pilot (Curtis) to 'feel out' the UAV and try to find its trim conditions. Curtis noted that there was a little wing rock but other than that it was pretty stable. Next the UAV was flown in trim down the length of the field. This went well and the UAV flew with an airspeed of 42.5 mph, which was on target with the design goal. Curt then performed left and right banked turns with a 30° bank angle. These banked turns were held for 10 seconds and were done at an airspeed of about 30 mph. There were no noticeable issues when performing the banked turns. The final test before land was finding the max speed for the UAV which was 67 mph. The landing was quite smooth with the only damage being done was the pitot tube breaking off and the control arm coming unhinged.

The second flight test was designed to test the performability of the UAV and to find out what happens when a control surface is failed briefly then recovered. To start the flight test a lift/drag glide was performed at a constant airspeed to check if it matched the expected value from design. While performing this glide Curtis noticed that when he increased throttle the UAV pitched up and when he decreased throttle it pitched down. This was due to the thrust line not being parallel to the UAV. The next test was finding the stall speed of the UAV and recovering. Unfortunately there was not enough elevator authority (did not deflect all the way) to cause the UAV to stall on purpose. The final test was to simulate a control surface failure by moving the joystick that controls the elevons diagonally which resulted in only one of the elevons to move. This was performed a few times with no noticeable immediate loss in stability. On landing the pitot tube broke off again.

Before the third test the pitot tube was moved to the top of the wing, washers were added to tilt the motor down (Figure 15), and the elevons were given full authority. The purpose of the third flight was to test the performance of the UAV operating with just one working control surface with the other failed in trim using an RX MUX. At the beginning of the flight it was noticed that thrust line was still not aligned but was performing better then before. When the control surface was failed the UAV remained stable and was able to be controlled for long lengths of time. No noticeable problems occurred when the control surface was failed except for a phugoid oscillation but it was not severe. The landing was done with both control surfaces operational and was very smooth. The only damage on land was that the pitot tube came a little loose but did not completely break off.

A fourth flight test was performed to find out if it was possible to land the UAV with a failed control surface. More washers had been added to point the motor down to adjust the thrust line and it was found to be good during the flight. Immediately after take off gusts of winds start appearing making it difficult to control the UAV with a failed control surface. Curtis had to abort landing several times due to problems controlling the UAV in the wind. On the final attempt Curtis was able to glide the UAV down safely to the ground. Since it was not possible to flare up while landing with only one control surface the impact was a little harder but still o.k. Unfortunately on landing the UAV missed the grass field and landed on clumpy dirt. Damage was minimal to the UAV with the pitot tube broken off and the wire connection was severed, another wire connection was severed inside the fuselage, and the skin on the leading edge of the starboard wing was scuffed up. No serious damage was done and everything was repairable.

References

- [1] Pae, Peter. "Boeing Developing Wing-Body Aircraft." Los Angeles Times. N.p., 9 Feb. 2001. Web. 2 May 2016.
- [2] Lednicer, David. "The Incomplete Guide to Airfoil Usage." UIUC Applied Aerodynamics Group. University of Illinois at Urbana - Champaign, 15 Sept. 2010. Web. 02 May 2016. <http://m-selig.ae.illinois.edu/ads/aircraft.html>.
- [3] "LA2573A." Airfoil Tools. Web. 02 May 2016. <http://airfoiltools.com/airfoil/detailsairfoil=la2573a-il>.
- [4] "Software Choice for Pixhawk Hardware." - Pixhawk Flight Controller Hardware Project. N.p., n.d. Web. 02 May 2016. <https://pixhawk.org/choice>.
- [5] <http://www.ecalc.ch/motorcalc.php>